Osmolyte-Mediated Encapsulation of Proteins inside MS2 Viral Capsids

Jeff E. Glasgow,[†] Stacy L. Capehart,[†] Matthew B. Francis,[†] and Danielle Tullman-Ercek[‡,*]

[†]Department of Chemistry, University of California, Berkeley, California 94720, United States and [‡]Department of Chemical and Biomolecular Engineering, University of California, Berkeley, California 94720, United States

ABSTRACT

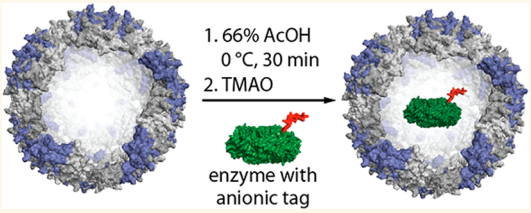

The encapsulation of enzymes in nanometer-sized compartments has the potential to enhance and control enzymatic activity, both *in vivo* and *in vitro*. Despite this potential, there is little quantitative data on the effect of encapsulation in a well-defined compartment under varying conditions. To gain more insight into these effects, we have characterized two improved methods for the encapsulation of heterologous molecules inside bacteriophage MS2 viral capsids. First, attaching DNA oligomers to a molecule of interest and incubating it with MS2 coat protein dimers yielded reassembled capsids that packaged the tagged molecules. The addition of a protein-stabilizing osmolyte, trimethylamine-*N*-oxide, significantly increased the yields of reassembly. Second, we found that expressed proteins with genetically encoded negatively charged peptide tags could also induce capsid reassembly, resulting in high yields of reassembled capsids containing the protein. This second method was used to encapsulate alkaline phosphatase tagged with a 16 amino acid peptide. The purified encapsulated enzyme was found to have the same K_m value and a slightly lower k_{cat} value than the free enzyme, indicating that this method of encapsulation had a minimal effect on enzyme kinetics. This method provides a practical and potentially scalable way of studying the complex effects of encapsulating enzymes in protein-based compartments.

KEYWORDS: virus · encapsulation · enzyme catalysis · nanoscience · compartmentalization

Recent research has shown that the confinement of biochemical reactions within nanometer-sized compartments can have a profound effect on enzymatic reaction rate and selectivity.[1,2] Many types of cells from all kingdoms of life are known to compartmentalize enzymes to take advantage of local environment effects, channeling, and substrate control.[3,4] Notable examples thought to capitalize on these advantages include bacterial microcompartments, such as the carbon-fixing carboxysome.[5] Due to their common occurrence, there is a growing interest in mimicking such systems, both *in vitro* and *in vivo*, using enzymes encapsulated in viral capsids.[6−8] Encapsulating enzymes in such protein compartments and studying the effects on catalyzed reactions could advance our understanding of the advantages brought about by reaction space confinement or could be used to alter substrate selectivity through selective diffusion through the shell.[9,10]

Recent approaches to the encapsulation of enzymes inside viral capsids have taken advantage of the reversible assembly of cowpea chlorotic mottle virus[11−13] and hepatitis B capsids,[14] triggered through changes in pH or salt concentration. This allows enzymes to be trapped inside. Other approaches have relied on specific interactions of fusion proteins with the bacteriophage P22 capsid[15,16] and simian virus 40[17] or of nucleic acids with the interior surfaces of bacteriophage Qβ.[18] The latter case provides a particularly elegant example, as the nucleic acid strands also possessed aptamer domains that bound to coexpressed proteins and packaged them *in vivo*. Nonviral protein shells have also been used to encapsulate proteins through electrostatic interactions both *in vivo*[19] and *in vitro*.[20]

Bacteriophage MS2 capsid has also been used extensively for virus-like particle applications, such as drug delivery,[21−23] MRI contrast enhancement,[24−26] and protein and nanoparticle encapsulation.[27,28] Many of these applications have capitalized on the presence of multiple ~2 nm pores, which allow small molecules to access the interior volume of the capsids, but are too small to allow folded proteins to pass through. This feature, in addition to unusually high stability of the MS2 capsid toward heat and denaturants, its tolerance of mutations, and its extensive structural characterization make it a particularly compelling protein shell for enzyme encapsulation.[29] Previous efforts to encapsulate heterologous molecules in the

* Address correspondence to dtercek@berkeley.edu.

Received for review May 17, 2012 and accepted September 6, 2012.

Published online September 06, 2012
10.1021/nn302183h

MS2 capsid have similarly taken advantage of a specific interaction of a short RNA oligonucleotide[30] with the interior surface of the capsid coat protein.[27] In this approach, RNA is attached to the molecule of interest, which is then mixed with capsid coat protein dimers to initiate assembly around the molecule to be encapsulated. This method has been used to encapsulate several kinds of molecules, including the ricin A chain, fluorescent quantum dots, doxorubicin, and anticyclin siRNAs;[28] however, the cost and instability of the RNA used limits the practicality of encapsulation on larger synthetic scales.

In this work, a convenient new osmolyte-based method is reported for cargo encapsulation using MS2 viral capsids. Osmolytes are a large class of small, neutral organic molecules often used by cells to regulate osmotic pressure,[31] with common examples including methylamines, polyols, and amino acids. These molecules can have a profound effect on protein stability and solubility; for example, urea is well-known to solubilize proteins while stabilizing the unfolded state.[32] Trimethylamine *N*-oxide (TMAO) is a common osmolyte often found in urea-rich organisms, which counteracts urea's effects.[33,34] As a result, the presence of TMAO can decrease unfolding while *increasing* the thermal stability of a wide variety of proteins.[35]

Herein we demonstrate that the attachment of DNA to a molecule of interest and incubation with MS2 coat protein (MS2-CP) dimers initiates reassembly around the molecule, similar to Ashley *et al.*,[28] but with a significantly more convenient packaging signal. The replacement of RNA with DNA greatly reduces cost while increasing nucleic acid stability, making large-scale encapsulation more feasible. Second, we show that addition of a genetically encoded poly(anionic) tag to a protein of interest also initiates reassembly and allows encapsulation. This method is advantageous, as the target protein requires no further *in vitro* modification and can be fully characterized before encapsulation. This latter method was used to encapsulate derivatives of green fluorescent protein and *E. coli* alkaline phosphatase. The encapsulated alkaline phosphatase retained its activity, with kinetic parameters nearly equal to those of the free enzyme. All these processes are possible through the addition of a stabilizing osmolyte, trimethylamine *N*-oxide.

RESULTS AND DISCUSSION

To develop a simple method of heterologous molecule encapsulation inside the MS2 capsid, we first attempted to initiate assembly of coat protein dimers using different oligonucleotides using similar conditions to those previously reported[27] (Figure 1a). Extended incubation of MS2-CP dimers (15 μM, based on monomer) with yeast tRNA or the 20 nucleotide DNA sequence corresponding to the MS2 translational repressor sequence[30] ("TR-DNA", Figure 1c) at various

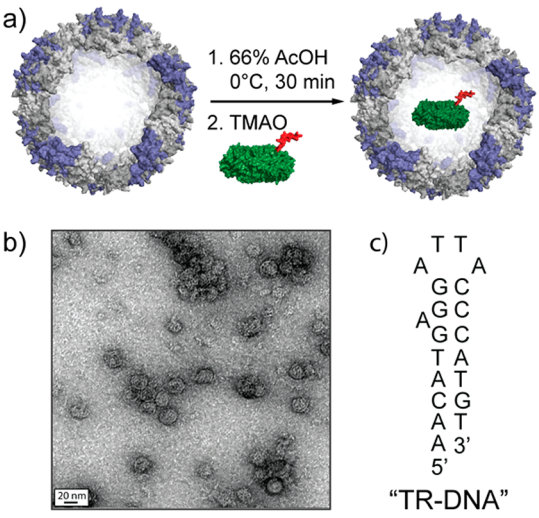

Figure 1. Bacteriophage MS2 reassembly process. (a) MS2 capsids are disassembled into dimers with acetic acid and centrifuged to remove RNA (ref 27). Reassembly is initiated with DNA, DNA conjugated molecules, or highly negatively charged molecues in the presence of trimethyl amine *N*-oxide (TMAO). Shown is a model of *E. coli* alkaline phosphatase (green) with a negatively charged peptide tag (red). (b) TEM image of reassembled MS2 capsids stained with $UO_2(OAc)_2$ (scale bar = 20 nm). (c) DNA sequence TR in predicted hairpin (ref 30). MS2 PDB 1ZDQ, alkaline phosphatase modeled from PDB 1ED8.

concentrations resulted in visible aggregation of the coat protein and little to no capsid formation, as measured by size exclusion chromatography (SEC). To stabilize the coat proteins and suppress aggregation, we repeated the experiments in the presence of various osmolytes, such as glycine, arginine, proline, urea, guanidinium chloride, and TMAO. The resulting protein was analyzed by SEC (Supplementary Figure S1). As shown in Figure 2a, increasing concentrations of TMAO in the presence of 50 μM TR-DNA led to increased yields of intact capsid. Similar results were obtained when TR-DNA was replaced with yeast tRNA (Supplementary Figure S1). Dynamic light scattering (DLS) of the reassembled capsid indicated a particle diameter of 27 nm, and transmission electron microscopy (TEM) images showed spherical particles matching untreated capsids (Supplementary Figure S2).

Interestingly, high concentrations of the osmolyte alone could also induce capsid reassembly, although the yield was greatly increased with the addition of TR-DNA. At even higher concentrations of TMAO, the yield of reassembled capsid decreased, probably due to a "salting out" effect (TMAO is known to decrease protein solubility at high concentrations[36]). Although the RNA translational repressor sequence has been shown to trigger capsid reassembly specifically,[37] we found that in the presence of TMAO, a random DNA sequence could also induce reassembly (Supplementary Figure S1). At higher TR-DNA concentrations, the reassembly yields were reduced. A similar effect has been observed in TR-RNA-induced reassembly experiments, where binding

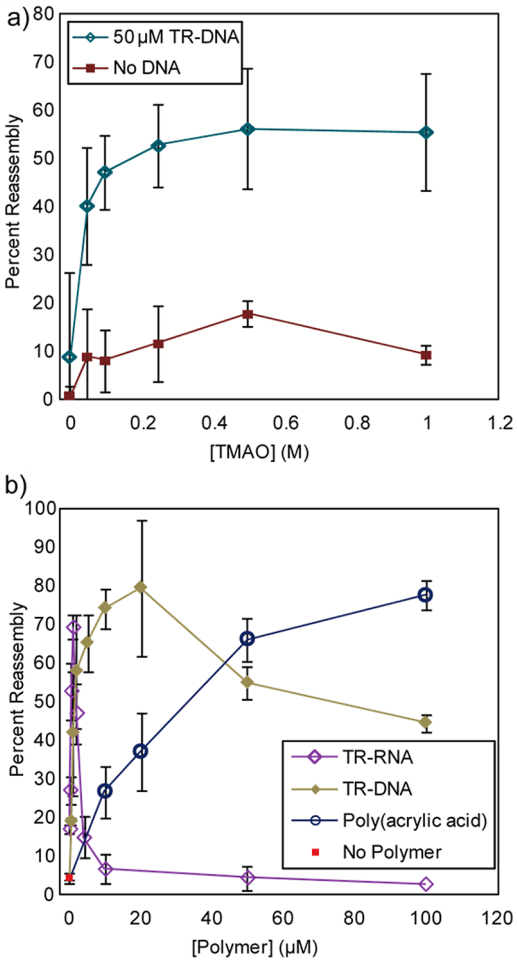

Figure 2. Encapsulation based on negative charge. (a) Reassembly occurs with increasing concentrations of TMAO in the presence and absence of TR-DNA. (b) Reassembly is enhanced with increasing concentrations of TR-DNA, TR-RNA, and poly(acrylic acid) 1.8k.

kinetically traps a significant pool of the capsid dimers in a nonassembling conformation.[38] For comparison, TR-RNA was also used to initiate reassembly. Also shown in Figure 2a is the TR-RNA-induced maximum reassembly at low micromolar concentrations, followed by a decrease in yield at higher TR-RNA levels. The difference between optimal TR-RNA and TR-DNA concentrations can be attributed to specific interactions between the coat protein and 2′-OH groups on TR-RNA, giving the RNA higher affinity.[39]

Previous studies have shown that negatively charged polymers can initiate viral capsid assembly and even induce the formation of previously uncharacterized structures.[40,41] There is evidence that other capsids from the *Leviviridae* family can assemble in this fashion, but little is known about the interaction of MS2-CP with anionic polymers.[42] To test whether a negatively charged polymer could initiate MS2 reassembly, disassembled coat protein was incubated with varying amounts of 1.8k poly(acrylic acid) and 0.25 M TMAO at pH 7.2. This polymer has approximately 20 acidic monomers and, at this pH, should have a significant negative charge. Similar to the TR-DNA, the poly(acrylic acid) was also found to induce significant amounts of reassembly in the presence of TMAO (Figure 2b). Presumably, the electrostatic attraction between the negatively charged molecules and the positively charged interior surface of the capsid initiated reassembly with the negative charge inside. At the concentrations used, the inhibitory effect seen with a large excess of TR-DNA was not observed.

On the basis of these experiments, we emerged with three options for the encapsulation of proteins inside the MS2 capsid: (1) the covalent attachment of a negatively charged polymer, such as DNA, RNA, or poly(acrylic acid), to a cargo group and using the conjugate to initiate reassembly; (2) the genetic addition of a negatively charged amino acid sequence to the protein of interest and using the purified protein to initiate reassembly; or (3) the use of naturally negatively charged proteins to reassemble the capsid.

Before encapsulating enzymes, we first attempted to encapsulate GFP as an easily detectable model protein. The monomeric form of enhanced GFP (mEGFP)[43,44] has a charge of approximately −7 at pH 7.2. Incubation of free mEGFP with disassembled capsid resulted in reassembly of less than 10% of the capsid dimers. Based on a comparison of the fluorescence of the MS2 tryptophans and the GFP fluorophore, there were approximately five GFP molecules per capsid.

To attach DNA to GFP we used an oxidative coupling strategy developed in our group (Figure 3a).[44] TR-DNA with a 5′ amino group was incubated with *N,N*-diethyl-*N*′-acylphenylenediamine NHS ester **1** to yield TR-DNA containing a phenylene-diamine moiety (**2**). GFP was incubated with isatoic anhydride to install an aniline derivative on surface lysine residues. The phenylene-diamine-containing TR-DNA was then incubated with the aniline GFP in the presence of 5 mM $NaIO_4$ for 1 h to yield GFP−DNA conjugate **3** in 35% yield by densitometry (Supplementary Figure S3). After purification by anion exchange FPLC, the conjugate was analyzed by SDS-PAGE (Figure 3b), confirming a shift in mass of about 6 kDa, corresponding to the TR-DNA attachment.

The GFP−DNA conjugate was next incubated with disassembled capsids in the presence of 0.25 M TMAO, as described above. After incubation the free GFP was purified away using 100 kDa spin concentrators. The GFP−DNA conjugate was able to initiate, on average, 35% (±6%, $n = 3$) of the MS2-CP dimers to assemble. As shown in Figure 3c, a significant amount of GFP fluorescence coeluted with the MS2 capsid. No such peak was seen when GFP and MS2 were co-injected, implying that the GFP−DNA was trapped inside the capsid when it was used to initiate reassembly. Based on the fluorescence of GFP eluting with the capsid, there was an average of 6.5 ± 1.9 GFP molecules per capsid.

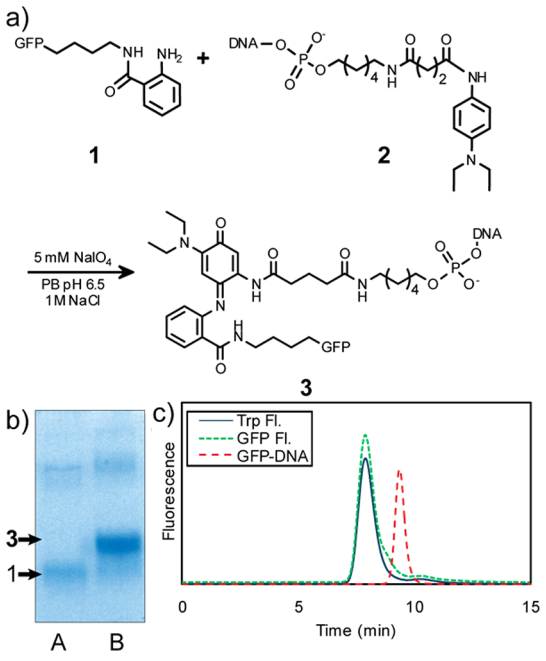

Figure 3. DNA–protein bioconjugation for encapsulation experiments. (a) mEGFP (40 μM, 10 mM PB pH 8.0) was incubated with isatoic anhydride (1 mM) for 1 h at room temperature to yield aniline-GFP 1. Phenylene diamine DNA 2 (ref 44) was incubated with 1 in 25 mM PB pH 6.5 with 5 mM $NaIO_4$ for 1 h to yield 3. (b) The DNA bioconjugation reaction was followed using SDS-PAGE (Coomassie stain). Lane A: Unreacted mEGFP; lane B: GFP–DNA conjugate 3. (c) HPLC trace of MS2 with encapsulated (green) and free (red) GFP–DNA.

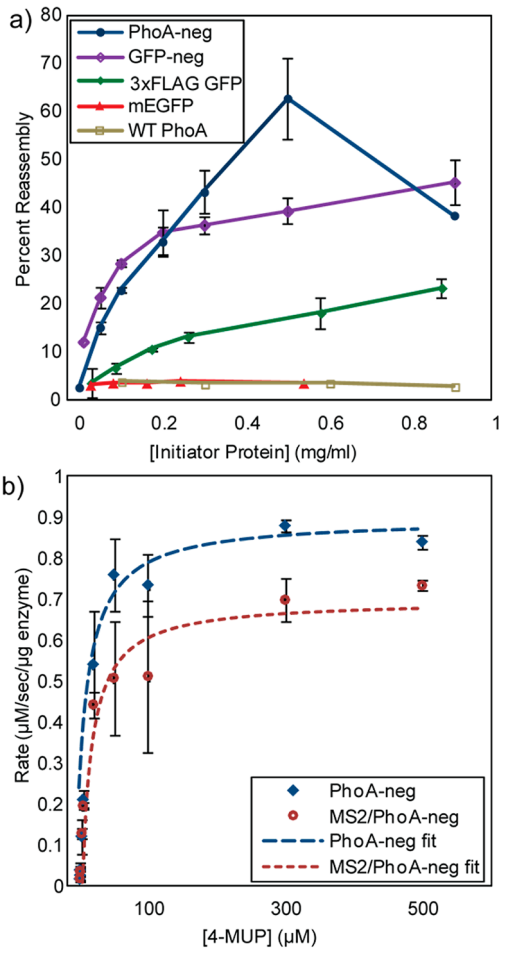

Kinetic Parameters

	K_m (μM)	k_{cat} (s^{-1})	k_{cat}/K_m ($M^{-1}s^{-1}$)
Free PhoA-neg	14.3	17.9	1.25×10^6
Encapsulated	14.5	14.0	9.6×10^5

Figure 4. Negatively charged protein encapsulation. (a) Reassembly yield with increasing concentrations of PhoA-neg (n = 2), 3xFLAG GFP (n = 2), His-GFP-neg (n = 3), mEGFF (n = 1), and wild-type PhoA (n = 1) in 0.25 M TMAO. (b) Rate profiles of free (red) *vs* MS2 encapsulated (blue) alkaline phosphatase dimer. The lines show the result of fitting the data to the Michaelis–Menten equation.

This corresponds roughly to a concentration of 2 mM GFP within the capsid volume.

To test if the addition of a negatively charged amino acid tag would enable the encapsulation of mEGFP, we next added a 3xFLAG tag to the N-terminus. As shown in Figure 4a, increasing amounts of 3xFLAG mEGFP corresponded to higher yields of capsid reassembly, whereas mEGFP gave low reassembly yield at all concentrations. Incorporation of mEGFP fluorescence into the capsid was confirmed by SEC-HPLC. To support the observation that negative charge was responsible for capsid reassembly, disassembled capsids were incubated with lysozyme (a well-known basic protein) and poly(ethylene glycol) 8k (a neutral polymer). Neither of these experiments resulted in significant amounts of reassembled capsid (Supplementary Figure S4). We then increased the negative charge by adding a C-terminal acidic peptide tag, inserting arbitrarily chosen codons for aspartate and glutamate residues (EEEEDDDEDDDDEEDD). An N-terminal 6xHis tag was also added for purification purposes. Reassembly of MS2-CP dimers with this construct, referred to as His-GFP-neg, is also shown in Figure 4a. Yield of intact capsid increased significantly using this construct, presumably due to the higher negative charge of the neg tag over the 3xFLAG tag (16 *vs* 9 total charges added). With an effective encapsulation strategy developed, we then proceeded to enzyme encapsulation.

E. coli alkaline phosphatase (PhoA) exists as a homodimer of a 49 kDa protein. After *in vivo* secretory processing,[45] each monomer is predicted to have a charge of approximately −8.6 at pH 7.2, giving the holoenzyme an approximate charge of −17. Incubation of MS2 coat protein dimers with free wild-type enzyme in the presence of TMAO resulted in low (<10%) yield of the reassembled capsid. To increase the yield of MS2-encapsulated PhoA, a large acidic peptide (EEEEDDDEDDDDEEDD) was added to the C-terminus (PhoA-neg). As shown in Figure 4a, increasing amounts of PhoA-neg incubated with disassembled

capsid resulted in increasing reassembly in a concentration-dependent fashion. At higher PhoA-neg concentrations, PhoA-neg inhibited capsid reassembly, possibly due to an undesired association between the large, dimeric enzyme and the positively charged MS2-CP surface, blocking assembly. The reassembled capsid was precipitated using a solution of 10% PEG 8k and 500 mM NaCl, and the obtained material was resuspended in ST buffer and purified by size exclusion HPLC. Fractions containing the intact capsids were collected and found to possess significant alkaline phosphatase activity, whereas corresponding fractions collected when preincubated mixtures of untreated, intact capsids and alkaline phosphatase were injected contained no activity (Supplementary Figure S5). A sample of the isolated capsids was analyzed using SDS-PAGE. Densitometry analysis after Coomassie staining indicated an average of 1.6 PhoA-neg dimers per capsid, corresponding to an effective enzyme concentration of 0.5 mM. The lower incorporation of PhoA-neg molecules per capsid, as compared to His-GFP-neg, is probably due to the enzyme's larger size and dimerization.

The kinetics of the encapsulated PhoA-neg were assayed by monitoring the hydrolysis of 4-methylumbelliferyl phosphate to yield fluorescent 4-methylumbelliferone in 100 mM 3-(*N*-morpholino)propanesulfonic acid buffer with 500 mM NaCl. As shown in Figure 4b, the encapsulated enzyme dimer followed Michaelis–Menten kinetics with a K_m equal to that of the free enzyme dimer. The k_{cat} was slightly reduced when the enzyme was encapsulated, possibly due to the constrained enzyme environment. Alkaline phosphatase is known to be a "nearly perfect" enzyme[46] and, therefore, is more susceptible to inhibited diffusion, but this did not appear to be the case here. Previous studies have shown both enhanced[13] and inhibited[18] kinetics for viral capsid based enzyme nanoreactor systems, suggesting that complex influences are operational in these systems. Other encapsulation systems based on liposome- or polymersome-encapsulated enzymes have shown similar variations in kinetic effects.[47,48] These systems are often complicated by permeability issues and undesirable enzyme conditions during synthesis. Because of the synthetic ease of this system, mild encapsulation conditions used, and modest effect on enzyme activity, MS2-encapsulated enzymes have the potential to elucidate the rich kinetic effects associated with confined enzyme compartments.

CONCLUSION

In summary, we have demonstrated two improved methods for encapsulating proteins inside MS2 capsids using a protein-stabilizing osmolyte to increase yields. In the first method, the capsid is reassembled around a protein of interest by means of a conjugated negatively charged polymer. DNA and poly(acrylic acid) are cheaper and more stable than RNA and offer a much more practical trigger for reassembly. The use of these polymers is not limited to protein encapsulation; any molecule larger than the MS2 capsid pores can be attached to a polymer *via* a wide variety of different conjugation reactions and used to trigger assembly. Our second method uses genetically encoded, negatively charged amino acid tags to specifically incorporate purified proteins into the capsid. This method allows facile encapsulation of enzymes into an easily modified protein shell, which will aid in studies on the precise effect that encapsulation has on enzyme activity, stability, and specificity. Furthermore, by altering the pore characteristics of the capsids, it may be possible to confer additional substrate selectivity or restrict the diffusion of inhibitory molecules. In this way, we intend to use this versatile encapsulation system to study electrostatic and steric effects on substrate diffusion into the capsid nanoreactor.

METHODS

Unless otherwise noted, all chemical reagents were purchased from Aldrich. For specific instrumentation and detailed experimental information see the Supporting Information.

MS2 Capsid Expression, Purification, and Disassembly. Wild-type bacteriophage MS2 capsids were expressed and purified as previously described.[25] Protein concentrations were determined using a BCA assay (Pierce). The capsids were disassembled using the method of Wu *et al.*[27] Briefly, a 10 mg/mL solution of intact MS2 capsids in ST buffer (50 mM Tris, 100 mM NaCl) was mixed with cold glacial acetic acid to give a final concentration of 66% acid. The mixture was incubated on ice for 30 min, then centrifuged at 16000*g* for 20 min at 4 °C to remove any nucleic acid contaminants. The supernatant was then desalted into 1 mM acetic acid using commercially available gel filtration columns (NAP-5, GE Healthcare). Fractions containing the disassembled capsid were maintained on ice and used on the same day.

Determination of Capsid Reassembly. The extent of capsid reassembly was determined by size exclusion chromatography on either a Polysep 5k column (capsids elute at 8.2 min at 1 mL/min flow rate) or Biosep 4k (capsids elute at 6.2 min at 1 mL/min flow rate). Tryptophan fluorescence (ex 280/em 330 nm) was tracked, and the area under the MS2 capsid peak was used to quantify concentration. Reassembled capsids were compared to intact capsid standards for absolute quantification. Typical chromatograms of various reassembly experiments are shown in Figure S1. Reassembled capsids were also analyzed by TEM and DLS (Supplemental Figure S2). To show the necessity of negative charge in reassembly, disassembled CP was incubated with lysozyme from chicken egg white type VI (MP Biomedicals, Solon, OH, USA) at several concentrations. No reassembly above background was observed (Supplemental Figure S3).

PhoA-neg Encapsulation and Purification. PhoA-neg (10 μM) was incubated for 36–48 h with disassembled MS2 (15 μM monomer concentration) in the presence of 0.25 M TMAO in ST buffer. The solution was then centrifuged at 10000*g* for 10 min. To the supernatant was added PEG 8k to 10% w/v and NaCl to a concentration of 0.5 M. The solution was rotated on a benchtop

rocker at 4 °C for 2 h and centrifuged at 17800*g* for 45 min. The resulting pellet was resuspended in a minimal amount of ST buffer and again spun at 10000*g* for 10 min. The supernatant was then applied to a Biosep SEC-S-4000 using a flow rate of 1 mL/min ST buffer. Fractions corresponding to intact MS2 capsids were collected, concentrated, and stored at 4 °C. Fractions were collected (1 min fractions at 1 mL/min) and assayed for hydrolysis of *p*-nitrophenyl phosphate in 1 M Tris-HCl, 10 μM $MgCl_2$, and 1 μM $ZnCl_2$. As controls, intact capsids were also incubated with PhoA-neg and purified and assayed in a similar manner. As shown in Supplemental Figure S5, no detectable phosphatase activity was associated with the intact capsid fractions without using the disassembly/reassembly protocol, implying that PhoA-neg was not associating with the outside of the capsids and co-purifying on the column. A small amount of free PhoA-neg precipitated with the capsids, but was fully purified away by SEC.

Alkaline Phosphatase Activity Assays. Alkaline phosphatase activity was characterized in two ways. First, the liberation of *p*-nitrophenol from *p*-nitrophenylphosphate in 1 M Tris pH 8.0, 10 mM $MgSO_4$, and 10 mM $ZnCl_2$ was followed using the absorbace at 405 nm. Second, the liberation of 4-methylumbelliferone from 4-methylumbelliferyl phosphate was followed in 0.1 M 3-(*N*-morpholino)propanesulfonic acid and 500 mM NaCl (ex. 362/em 448 nm).

Conflict of Interest: The authors declare no competing financial interest.

Acknowledgment. J.G., M.F., and D.T.-E. are affiliated with the Energy Biosciences Institute. J.E.G. was supported by the U. C. Berkeley Chemical Biology Graduate Program (NIH Training Grant 1 T32 GMO66698).

Supporting Information Available: Additional methods details; additional MS2 capsid characterization figures including transmission electron micrographs, dynamic light scattering, and chromatography traces; additional TR-DNA GFP conjugation figure including protein gel and chromatography traces. This material is available free of charge *via* the Internet at http://pubs.acs.org.

REFERENCES AND NOTES

1. Kim, K. T.; Meeuwissen, S. A.; Nolte, R. J. M.; van Hest, J. C. M. Smart Nanocontainers and Nanoreactors. *Nanoscale* **2010**, *2*, 844–858.
2. Vriezema, D.; Comellas-Aragonès, M.; Elemans, J.; Cornelissen, J. J. L. M.; Rowan, A. E.; Nolte, R. J. M. Self-Assembled Nanoreactors. *Chem. Rev.* **2005**, *105*, 1445–1490.
3. Huang, X.; Holden, H. M.; Raushel, F. M. Channeling of Substrates and Intermediates in Enzyme-Catalyzed Reactions. *Annu. Rev. Biochem.* **2001**, *70*, 149–180.
4. Yeates, T.; Kerfeld, C.; Heinhorst, S.; Cannon, G.; Shively, J. Protein-Based Organelles in Bacteria: Carboxysomes and Related Microcompartments. *Nat. Rev.* **2008**, *6*, 681–691.
5. Kinney, J. N.; Axen, S. D.; Kerfeld, C. A. Comparative Analysis of Carboxysome Shell Proteins. *Photosynth. Res.* **2011**, *109*, 21–32.
6. de la Escosura, A.; Nolte, R. J. M.; Cornelissen, J. J. L. M. Viruses and Protein Cages as Nanocontainers and Nanoreactors. *J. Mat. Chem.* **2009**, *19*, 2274–2278.
7. Conrado, R. J.; Varner, J. D.; DeLisa, M. P. Engineering the Spatial Organization of Metabolic Enzymes: Mimicking Nature's Synergy. *Curr. Opin. Biotechnol.* **2008**, *19*, 492–499.
8. Aniagyei, S. E.; DuFort, C.; Kao, C. C.; Dragnea, B. Self-Assembly Approaches to Nanomaterial Encapsulation in Viral Protein Cages. *J. Mater. Chem.* **2008**, *18*, 3763–3774.
9. Conrado, R. J.; Mansell, T. J.; Varner, J. D.; DeLisa, M. P. Stochastic Reaction-Diffusion Simulation of Enzyme Compartmentalization Reveals Improved Catalytic Efficiency for a Synthetic Metabolic Pathway. *Metab. Eng.* **2007**, *9*, 355–363.
10. Renggli, K.; Baumann, P.; Langowska, K.; Onaca, O.; Bruns, N.; Meier, W. Selective and Responsive Nanoreactors. *Adv. Func. Mater.* **2011**, *21*, 1241–1259.
11. Comellas-Aragonès, M.; Engelkamp, H.; Claessen, V. I.; Sommerdijk, N. A. J. M.; Rowan, A. E.; Christianen, P. C. M.; Maan, J. C.; Verduin, B. J. M.; Cornelissen, J. J. L. M.; Nolte, R. J. M. A Virus-Based Single-Enzyme Nanoreactor. *Nat. Nanotechnol.* **2007**, *2*, 635–639.
12. Minten, I. J.; Wilke, K. D. M.; Hendriks, L. J. A.; van Hest, J. C. M.; Nolte, R. J. M.; Cornelissen, J. J. L. M. Metal-Ion-Induced Formation and Stabilization of Protein Cages Based on the Cowpea Chlorotic Mottle Virus. *Small* **2011**, *7*, 911–919.
13. Minten, I. J.; Claessen, V. I.; Blank, K.; Rowan, A. E.; Nolte, R. J. M.; Cornelissen, J. J. L. M. Catalytic Capsids: The Art of Confinement. *Chem. Sci.* **2011**, *2*, 358–362.
14. Lee, K. W.; Tan, W. S. Recombinant Hepatitis B Virus Core Particles: Association, Dissociation and Encapsidation of Green Fluorescent Protein. *J. Virol. Meth.* **2008**, *151*, 172–180.
15. O'Neil, A.; Reichhardt, C.; Johnson, B.; Prevelige, P.; Douglas, T. Genetically Programmed *in Vivo* Packaging of Protein Cargo and Its Controlled Release from Bacteriophage P22. *Angew. Chem., Int. Ed.* **2011**, *50*, 7425–7428.
16. Patterson, D. P.; Prevelige, P. E.; Douglas, T. Nanoreactors by Programmed Enzyme Encapsulation Inside the Capsid of the Bacteriophage P22. *ACS Nano* **2012**, *6*, 5000–5009.
17. Inoue, T.; Kawano, M.; Takahashi, R.; Tsukamoto, H.; Enomoto, T.; Imai, T.; Kataoka, K.; Handa, H. Engineering of SV40-Based Nano-capsules for Delivery of Heterologous Proteins As Fusions with the Minor Capsid Proteins VP2/3. *J. Biotechnol.* **2008**, *134*, 181–192.
18. Fiedler, J. D.; Brown, S. D.; Lau, J. L.; Finn, M. G. RNA-Directed Packaging of Enzymes within Virus-Like Particles. *Angew. Chem., Int. Ed.* **2010**, *49*, 9648–9651.
19. Wörsdörfer, B.; Woycechowsky, K. J.; Hilvert, D. Directed Evolution of a Protein Container. *Science* **2011**, *331*, 589–592.
20. Wörsdörfer, B.; Pianowski, Z.; Hilvert, D. Efficient *in Vitro* Encapsulation of Protein Cargo by an Engineered Protein Container. *J. Am. Chem. Soc.* **2012**, *3*, 9–11.
21. Wu, W.; Hsiao, S. C.; Carrico, Z. M.; Francis, M. B. Genome-Free Viral Capsids as Multivalent Carriers for Taxol Delivery. *Angew. Chem., Int. Ed.* **2009**, *48*, 9493–9497.
22. Stephanopoulos, N.; Carrico, Z. Nanoscale Integration of Sensitizing Chromophores and Porphyrins with Bacteriophage MS2. *Angew. Chem., Int. Ed.* **2009**, 9498–9502.
23. Stephanopoulos, N.; Tong, G. J.; Hsiao, S. C.; Francis, M. B. Dual-Surface Modified Virus Capsids for Targeted Delivery of Photodynamic Agents to Cancer Cells. *ACS Nano* **2010**, *4*, 6014–6020.
24. Anderson, E. A.; Isaacman, S.; Peabody, D. S.; Wang, E. Y.; Canary, J. W.; Kirshenbaum, K. Viral Nanoparticles Donning a Paramagnetic Coat: Conjugation of MRI Contrast Agents to the MS2 Capsid. *Nano Lett.* **2006**, *6*, 1160–1164.
25. Meldrum, T.; Seim, K. L.; Bajaj, V. S.; Palaniappan, K. K.; Wu, W.; Francis, M. B.; Wemmer, D. E.; Pines, A. A Xenon-Based Molecular Sensor Assembled on an MS2 Viral Capsid Scaffold. *J. Am. Chem. Soc.* **2010**, *132*, 5936–5937.
26. Garimella, P. D.; Datta, A.; Romanini, D. W.; Raymond, K. N.; Francis, M. B. Multivalent, High-Relaxivity MRI Contrast Agents Using Rigid Cysteine-Reactive Gadolinium Complexes. *J. Am. Chem. Soc.* **2011**, *133*, 14704–14709.
27. Wu, M.; Brown, W.; Stockley, P. Cell-Specific Delivery of Bacteriophage-Encapsidated Ricin A Chain. *Bioconjugate Chem.* **1995**, 587–595.
28. Ashley, C. E.; Carnes, E. C.; Phillips, G. K.; Durfee, P. N.; Buley, M. D.; Lino, C. A.; Padilla, D. P.; Phillips, B.; Carter, M. B.; Willman, C. L.; *et al*. Cell-Specific Delivery of Diverse Cargos by Bacteriophage MS2 Virus-Like Particles. *ACS Nano* **2011**, *5*, 5729–5745.
29. Stonehouse, N.; Stockley, P. Effects of Amino Acid Substitution on the Thermal Stability of MS2 Capsids Lacking Genomic RNA. *FEBS Lett.* **1993**, *334*, 355–359.
30. Beckett, D.; Uhlenbeck, O. C. Ribonucleoprotein Complexes of R17 Coat Protein and a Translational Operator Analog. *J. Mol. Biol.* **1988**, *204*, 927–938.
31. Kumar, R. Role of Naturally Occurring Osmolytes in Protein Folding and Stability. *Arch. Biochem. Biophys.* **2009**, *491*, 1–6.
32. Bolen, D. W. Effects of Naturally Occurring Osmolytes on Protein Stability and Solubility: Issues Important in Protein Crystallization. *Methods* **2004**, *34*, 312–322.

33. Yancey, P. H.; Clark, M. E.; Hand, S. C.; Bowlus, R. D.; Somero, G. N. Living With Water Stress: Evolution of Osmolyte Systems. *Science* **1982**, *217*, 1214–1222.
34. Wang, A.; Bolen, D. A Naturally Occurring Protective System in Urea-Rich Cells: Mechanism of Osmolyte Protection of Proteins Against Urea Denaturation. *Biochemistry* **1997**, *36*, 9101–9108.
35. Street, T. O.; Bolen, D. W.; Rose, G. D. A Molecular Mechanism for Osmolyte-Induced Protein Stability. *Proc. Nat. Acad. Sci.* **2006**, *103*, 13997–14002.
36. Zhang, Y.; Cremer, P. S. Chemistry of Hofmeister Anions and Osmolytes. *Annu. Rev. Phys. Chem.* **2010**, *61*, 63–83.
37. ElSawy, K.; Caves, L.; Twarock, R. The Impact of Viral RNA on the Association Rates of Capsid Protein Assembly: Bacteriophage MS2 as a Case Study. *J. Mol. Biol.* **2010**, *400*, 935–947.
38. Rolfsson, O.; Toropova, K.; Ranson, N. A; Stockley, P. G. Mutually-Induced Conformational Switching of RNA and Coat Protein Underpins Efficient Assembly of a Viral Capsid. *J. Mol. Biol.* **2010**, *401*, 309–322.
39. Valegård, K.; Murray, J. B.; Stockley, P. G.; Stonehouse, N. J.; Liljas, L. Crystal Structure of an RNA Phage Coat Protein-Operator Complex. *Nature* **1994**, *371*, 623–626.
40. Douglas, T.; Young, M. Host−Guest Encapsulation of Materials by AssembledVirus Protein Cages. *Nature* **1998**, *393*, 1996–1999.
41. Hu, Y.; Zandi, R.; Anavitarte, A.; Knobler, C. M.; Gelbart, W. M. Packaging of a Polymer by a Viral Capsid: The Interplay Between Polymer Length and Capsid Size. *Biophys. J.* **2008**, *94*, 1428–1436.
42. Hohn, T. Role of RNA in the Assembly Process of Bacteriophage fr. *J. Mol. Biol.* **1969**, *43*, 191–200.
43. Zacharias, D. A.; Violin, J. D.; Newton, A. C.; Tsien, R. Y. Partitioning of Lipid-Modified Monomeric GFPs Into Membrane Microdomains of Live Cells. *Science* **2002**, *296*, 913–916.
44. Hooker, J. M.; Esser-Kahn, A. P.; Francis, M. B. Modification of Aniline Containing Proteins Using an Oxidative Coupling Strategy. *J. Am. Chem. Soc.* **2006**, *128*, 15558–15559.
45. Karamyshev, A. L.; Karamysheva, Z. N.; Kajava, A. V.; Ksenzenko, V. N.; Nesmeyanova, M. A. Processing of Escherichia coli Alkaline Phosphatase: Role of the Primary Structure of the Signal Peptide Cleavage Region. *J. Mol. Biol.* **1998**, *277*, 859–870.
46. Simopoulos, T. T.; Jencks, W. P. Alkaline Phosphatase is an Almost Perfect Enzyme. *Biochemistry* **1994**, *33*, 10375–10380.
47. Peters, R.; Louzao, I.; van Hest, J. C. M. From Polymeric Nanoreactors to Artificial Organelles. *Chem. Sci.* **2011**, *3*, 335–342.
48. Jesorka, A.; Orwar, O. Liposomes: Technologies and Analytical Applications. *Ann. Rev. Anal. Chem.* **2008**, *1*, 801–832.